JACS
JOURNAL OF THE AMERICAN CHEMICAL SOCIETY
Article
pubs.acs.org/JACS

Evidence for OH Radical Production during Electrocatalysis of Oxygen Reduction on Pt Surfaces: Consequences and Application

Jean-Marc Noël,[†] Alina Latus,[‡] Corinne Lagrost,[†] Elena Volanschi,[‡] and Philippe Hapiot*[,†]

[†]Sciences Chimiques de Rennes, UMR CNRS 6226, Université de Rennes 1, Equipe MaCSE, Campus de Beaulieu, 35042 Rennes Cedex, France

[‡]Department of Physical Chemistry, University of Bucharest, Boulevard Elisabeta 4-12, Bucharest 030018, Romania

ABSTRACT: Multielectronic O_2 reduction reactions (ORR) at Pt surface (and at Au surface for comparison purpose) were examined both in water and in organic solvents using a strategy based on radical footprinting and scanning electrochemical microscopy (SECM). Experiments reveal a considerable and undocumented production of OH radicals when O_2 is reduced at a Pt electrode. These observations imply that the generally admitted description of ORR as simple competitive pathways between 2-electron (O_2 to H_2O_2) and 4-electron (O_2 to H_2O) reductions is often inadequate and demonstrate the occurrence of another 3-electron pathway (O_2 to OH radical). This behavior is especially observable at neutral and basic pH's in water and in organic solvents like dimethylformamide or dichloromethane. In view of the high reactivity of OH radical versus organic or living materials, this observation could have important consequences in several practical situations (fuel cells, sensors, etc.) as far as O_2 reduction is concerned. This also appears as a simple way to locally produce highly reactive species as exemplified in the present work by the micropatterning of organic surfaces.

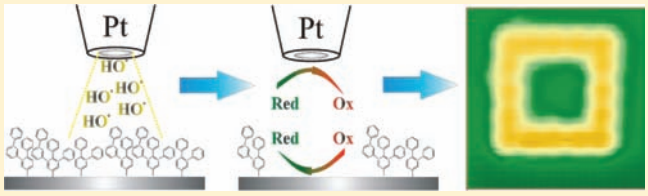

INTRODUCTION

Redox properties of dioxygen and derivatives are fundamental to understand many of the most important biological or chemical processes, but are also essential in modern applications such as fuel cells.[1,2] Numerous investigations have been carried out during these last decades and in the recent literature related to the oxygen reduction reaction (ORR).[1,2] The mechanism depends on the experimental conditions, solvent, or pH, but also on the nature of the electrode material in the case of heterogeneous reduction as in electrochemical catalysis. In aprotic solvents, oxygen is reduced to superoxide (reaction 1) contrarily to aqueous electrolyte or organic solvent in presence of acid where 2- or 4-electron reduction (reactions 2 or 3) are reported:[1,2]

$$O_2 + e^- \rightarrow O_2^{\bullet -} \quad (1)$$

$$O_2 + 2H^+ + 2e^- \rightarrow H_2O_2 \quad (2)$$

$$O_2 + 4H^+ + 4e^- \rightarrow 2H_2O \quad (3)$$

These global reactions do not reflect the mechanistic pathways. Other unstable and transient reactive oxygen species (ROS) play a key role even if they are not explicitly considered.[1] Detailed mechanistic studies have mainly focused on the two-electron process in aprotic solvents and on inert materials.[1−3] In the presence of added acid, it was demonstrated that the reduction first involves the formation of superoxide, $O_2^{\bullet -}$, then a proton transfer between $O_2^{\bullet -}$, acting as a weak base, and an acid AH (reaction 4).[3] Produced $HO_2^{\bullet}$ is more easily reduced than the starting superoxide and it rapidly exchanges a second electron at the electrode surface or in solution (ECE-DISP mechanism).[3]

$$O_2^{\bullet -} + AH \leftrightarrows HO_2^{\bullet} + A^- \quad (4)$$

$$HO_2^{\bullet} + O_2^{\bullet -} \rightarrow HO_2^- + O_2 \quad (5)$$

$$HO_2^{\bullet} + e^- \rightarrow HO_2^- \quad (6)$$

$$HO_2^- + AH \rightarrow H_2O_2 + A^- \quad (7)$$

More recently, mechanistic aspects of ORR were investigated in NaOH solutions where $O_2^{\bullet -}$ was found as the primary radical produced after electron transfer, suggesting similar first reaction steps in aqueous alkaline and in some organic solvents.[4]

The situation becomes much more complex when considering the following reduction steps possibly involved in a 4-electron mechanism. The role of water and other weak acids in the reduction of superoxide ions have been addressed, showing subtle media effects.[5] Reduction of H_2O_2 depends on the electrode material and solvent, but the global mechanism is unclear.[6] Disproportionation of H_2O_2 or its reduction has been proposed besides the metal oxide route for H_2O_2 evolution especially for reduction at metals like Pt.[6,7] We could also mention the possible occurrence of concerted proton−electron transfers[8] to oxygen and the reductive cleavage of O−O bond, especially when the surface displays active catalytic properties versus ORR.[9] The complexity of these processes combined with the transient character of ROS explains why the

Received: December 14, 2011
Published: January 12, 2012

 © 2012 American Chemical Society dx.doi.org/10.1021/ja211663t | J. Am. Chem.Soc. 2012, 134, 2835−2841

discrimination between mechanisms in ORR is difficult and often the implications of ROS like $HO_2^{\bullet}$ or $HO^{\bullet}$ in ORR remain elusive. In literature, discerning among the different ORR mechanisms is usually performed using steady state voltammetry (rotating disk electrode) providing an overall measure of the electronic stoichiometry.[1,10] Such a treatment assumes a combination of reactions 2 + 3 for ORR, meaning that the best catalyst is basically chosen as promoting the highest possible electronic stoichiometry (near 4 electrons). As explained before,[6b] this is a dangerous procedure based solely on a single parameter that neglects other possible reactions leading to the formation of different ROS during electrocatalysis. The production of ROS could often be indirectly detected through their effects on other molecules or materials. For example, $HO^{\bullet}$ radicals produced via Fenton reaction react with numerous materials and molecules and are efficiently used in environmental applications[11] or in local patterning of surfaces.[12] Surface mapping techniques using reactions with $HO^{\bullet}$ radicals are becoming increasingly popular for studying protein structure (radical footprinting techniques).[13] In this context, the development of local electrochemical methods like the Scanning Electrochemical Microscope (SECM) provides new possibilities thanks to the large variety of reacting agents that could be produced at a microelectrode and to the diversity of surfaces that could be investigated with this approach (conducting, semiconducting, or insulating interfaces).[14] For example, SECM in conjunction with ROS production have been considered in studying properties of electrogenerated intermediates,[14] in the evaluation of electrocatalysis efficiencies,[2] in the design of nano- or micropatterned functional surfaces without use of preformed mask,[12] or in direct relation with this work, in the quantification of oxide on gold and platinum electrode.[7a]

In the present work, we focused on the possible production of highly reactive oxygen species on noble metal surface through their ability to induce irreversible transformation of organic materials. Several consequences could be drawn from the present work that may lead to reevaluate experimental situations, when ORR is involved. Indeed, the controlled production of ROS could be highly advantageous when used as active reagents, but it becomes a significant problem when ROS are not desired. These observations also lead us to propose an easy and reproducible technique with minimum costs for patterning functional surfaces at the submicrometer scale.

EXPERIMENTAL SECTION

Chemicals (unless noted below) were commercially available and were purchased with the highest available purities. Benzenediazonium tetrafluoroborate, synthetized in aqueous acidic solution, was prepared from in an ice cold solution of the corresponding aniline (10^{-3} mol L^{-1}) in HBF_4 (48%) in which $NaNO_2$ (1.1×10^{-3} mol L^{-1}) dissolved in the minimum amount of water was slowly added. The precipitate was filtered, washed with ether, and dried in vacuum. 4-Aminomethylbenzylamine and potassium hexafluorophosphate (KPF_6) were from Acros. Potassium hydrogen phosphate and potassium dihydrogen phosphate, used for buffer solutions preparation (PBS), pH 7, were purchased from Alfa Aesar. Ultrapure water (18.2 MΩ cm) was used for preparation of the solutions. Hydroxymethylferrocene ($FcCH_2OH$) and tetrathiafulvalene (TTF) (97%) were purchased from Alfa-Aesar. Tetrabutylammonium hexafluorophosphate (NBu_4PF_6) and lithium perchlorate ($LiClO_4$) were obtained from Fluka. Absolute acetonitrile (ACN), dimethylformamide (DMF), dimethyl sulfoxide (DMSO), hydrogene peroxide (30%), and ethynylaniline (97%) were obtained from Sigma-Aldrich. Hydrochloric acid and ethanol anhydrous, EtOH, were received from Panseac and from Carlo ERBA, respectively. Tetrahydrofuran (THF), dichloromethane, and sodium hydroxide were from VWR.

SECM Experiments. Approach curves in feedback mode were recorded using a CHI910B instrument from CH-Instruments equipped with an adjustable stage for the tilt angle correction. The UME was a 5-μm radius Pt ultramicroelectrode (UME, CH Instruments) presenting typical RG of 10. The reference electrode was Ag/$AgNO_3$ and a Pt wire was used as a counter electrode. Approach curve consisted of recording the normalized current $I = I/I_{inf}$ that is plotted versus the normalized distance $L = d/a$ (where I is the current at the UME localized a distance d from the substrate). I_{inf} is the steady-state current when the UME is an infinite distance from the substrate: $I_{inf} = 4nFDCa$, where n is the number of electrons transferred per species, F is the Faraday constant, D and C are the diffusion coefficient and the initial concentration of the mediator, respectively, and a is the radius of the microelectrode.[14] All measurements were performed at room temperature. The feedback character of the approach curves (from a positive to a negative feedback) was characterized by the apparent electron transfer rate, k_{el}, derived from comparison with theoretical curves assuming an irreversible electron transfer at the sample and using recent semiempirical treatments.[14,15]

Atomic Force Microscopy (AFM). Contact-mode AFM measurements were performed with a PicoSPM II coupled with an interface Pico-SCAN 2500. The scanner used was a PicoSPM II 10 nm. Images were recorded with PicoSCAN software (version 5.3.3).

Surface Preparation and Electrografting Procedure. The 3-mm diameter glassy carbon (GC) disk (from CH Instruments, Austin, TX) serving as substrate were electro-modified by reduction of an aryldiazonium salt following the published procedures.[16] Before modification, the GC surface was cleaned, polishing successively with SiC paper 5 μm (Struers) and DP-Nap paper 1 μm (Struers). After each polishing step, electrodes were carefully washed with ultra pure water. The different aryldiazonium tetrafluoroborate salts (2×10^{-2} mol L^{-1}) dissolved in ACN/NBu_4BF_4 0.1 mol L^{-1} were reduced at constant potential of −1 V versus SCE for 10 min. Following the modification, each modified carbon surface was rinsed thoroughly and several times with ultra pure water. The long electrolysis time and the high value of potential allow the formation of thick multilayers at the carbon surface (thickness in the 10 nm range).[16,17]

RESULTS AND DISCUSSION

Oxygen Reduction in Water in Proximity with an Aromatic Substrate. We followed a footprint strategy based on the use of SECM in feedback mode and unbiased conditions.[14] O_2 is reduced at a tip electrode (Pt or Au) that is localized in the vicinity of a test substrate composed of a conducting substrate (glassy carbon) covered by an organic layer. In a second step, the local transformations of the layer are read with an indifferent redox mediator (see Scheme 1). Different types of approach curves are obtained (from positive to negative feedback) that sense the ability of the probe to pass through the layer, providing a view of the modifications. This strategy could be extended to a large variety of samples because the surface sample is not electrically connected. Our test surface (see Scheme 2) was a glassy carbon substrate on which different polyaromatic layers were covalently bound by electroreduction of aryldiazonium salt. Electrografting was performed under "self-inhibition" conditions (long-time electrolysis and with large concentration of precursor) with the purpose of obtaining thick layers with strong blocking properties.[16]

The obtained layer is principally composed of a condensation of aromatic rings (typical thickness in the 10 nm range) that are covalently bound to the carbon substrate.[16,17] These interfaces present large interests in many applications, but in our case, they are good examples of very robust organic layers in terms of mechanical and chemical stabilities.[16]

Scheme 1. Principle of the Radical Footprint SECM Analysis: (1 and 2) Positioning of the Tip Electrode near the Modified Surface; (3) Exposure of the Surface to ROS Production at the Tip Electrode; (4) Reading the Surface with an Indifferent Redox Probe

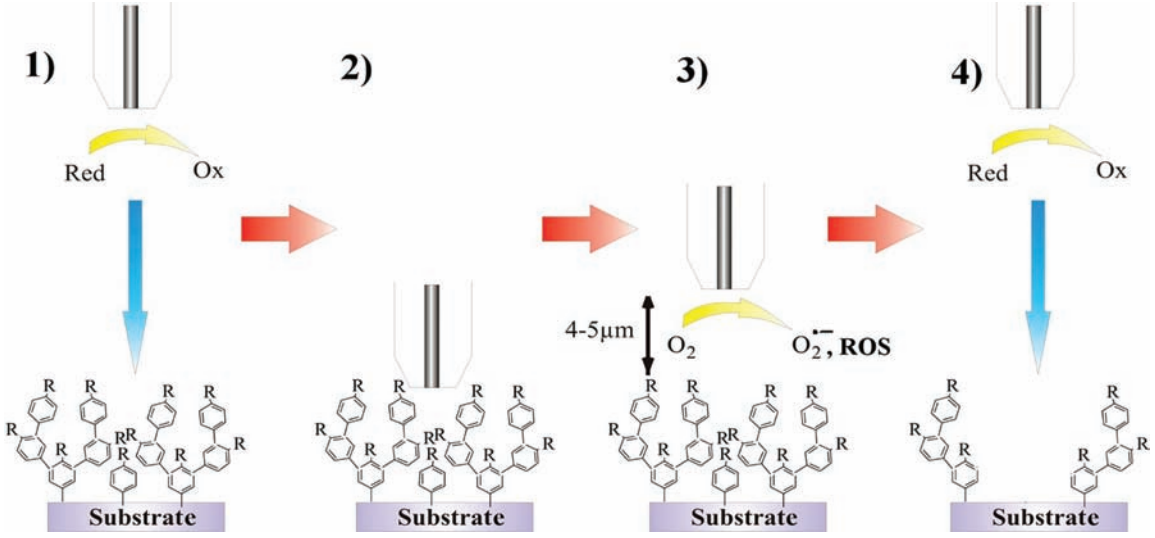

Scheme 2. Schematic Drawing of the Modified Surfaces Considered in This Work: (A) Polyphenylene-methylamine; (B) Polyphenylene-ethynyl; (C) Polyphenylene

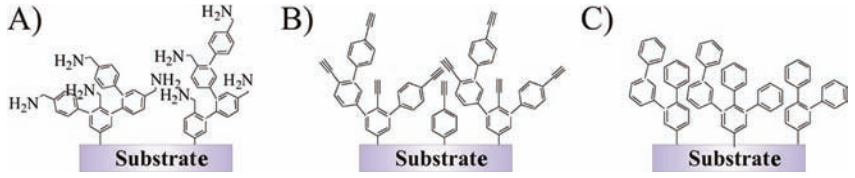

Each surface was first characterized by a SECM approach curve allowing an evaluation of its quality. Figure 1 (blue curve)

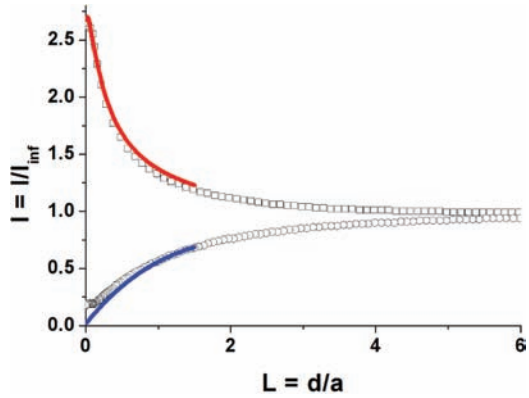

Figure 1. SECM approach curves (Pt UME, a = 5 μm) on modified GC electrode (polyphenylene layer C) in H_2O/KPF_6 0.1 mol L^{-1}: before (○) and after (□) exposure to O_2 reduction (2 × 10 s). $FcCH_2OH$ is used as a redox probe. Lines are the simulated curves for irreversible electron transfer kinetics. k_{el} = 3.1 × 10^{-4} cm s^{-1} (blue line), 5.2 × 10^{-2} cm s^{-1} (red line). d is the tip−substrate distance.

shows typical approach curves recorded on the modified surface C (polyphenylene layer)[16] in aqueous solution and using hydroxymethylferrocene ($FcCH_2OH$) as a redox probe. The approach curve displays a negative feedback indicating that the redox probe could not pass through the organic layer to reach the carbon substrate. This observation corresponds to an insulating surface behavior, which is expected for glassy carbon surfaces modified by electrografting of aryldiazonium under self-inhibition conditions.[17]

The SECM technique is then used to evaluate the reactivity of electrogenerated ROS. As shown in Scheme 1, oxygen dissolved in water is reduced at the tip electrode that is positioned near the modified carbon substrate (at a distance around the radius of the tip electrode).[18] Two tip electrodes were considered: gold and platinum microelectrodes, Pt because of its implications in analytical devices or as catalyst for ORR[2,4] and Au as a reference system. The O_2 solution contains also a redox probe ($FcCH_2OH$) that is used to position the tip electrode and allows the examination of the locally affected area without moving the tip. When the tip electrode was a gold microelectrode, the examination of the surface with the SECM approach curves did not show any modification even after a prolonged exposure to O_2 reduction. On the contrary, when a Pt microelectrode was used for O_2 reduction, the approach curves recorded with $FcCH_2OH$ reveal considerable modifications of the surface as illustrated with a positive feedback (compare curves blue and red in Figure 1). It indicates that the redox probe could easily reach the carbon substrate and thus, that the organic layer has been locally destroyed by species produced at the Pt tip electrode during O_2 reduction. Similar results were obtained with the three modified surfaces A−C shown in Scheme 2.

Oxygen Reduction in Organic Solvents in Proximity with an Aromatic Substrate. As complement to investigations in water, SECM experiments were achieved in several aerated organic solvents. Figure 2 illustrates the effects of oxygen reduction on the modified surface in different classical solvents: ethanol (EtOH/$LiClO_4$ 0.1 mol L^{-1}), dimethylsulfoxide

dx.doi.org/10.1021/ja211663t | J. Am. Chem.Soc. 2012, 134, 2835−2841

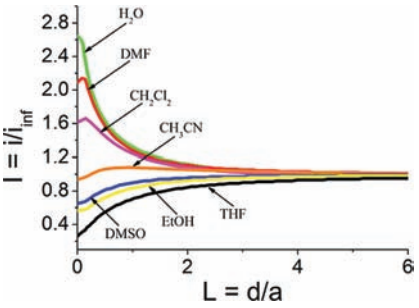

Figure 2. Solvent effect. Approach curves using $FcCH_2OH$ 10^{-3} mol L^{-1} as redox probe after exposure to O_2 reduction (2 × 10 s) on a 5 μm radius disk Pt tip electrode in the different solvents.

($DMSO/NBu_4PF_6$ 0.1 mol L^{-1}), tetrahydrofuran (THF/NBu_4PF_6 0.1 mol L^{-1}), acetonitrile (ACN/NBu_4PF_6 0.1 mol L^{-1}), dichloromethane (DCM/NBu_4PF_6 0.1 mol L^{-1}), and dimethylformamide (DMF/NBu_4PF_6 0.1 mol L^{-1}).

For each solvent, the destructive effect of the ROS on the organic film was evaluated by examining the SECM response with $FcCH_2OH$ in the same solvent. In THF, EtOH, and DMSO, very little or no changes on the substrate are visible. The largest transformations are observed when the process is performed in DMF and H_2O, leading to the global ranking: THF < EtOH < DMSO < ACN < DCM < DMF < H_2O (pH 7.4). Remarkably, when the tip electrode was an Au electrode, no modification of the surfaces was detected in any of the solvents considered in the study.

What Are the Species Responsible for This Reactivity?

A central question concerns the nature of the species produced at the tip electrode reacting with the polyphenyl layer. Multielectronic ORR may lead to the formation of numerous ROS species depending on media and electrode. Some ROS are extremely reactive such as the hydroxyl radical ($HO^{\bullet}$),[19] reactive like the hydroperoxyl radical ($HO_2^{\bullet}$) and H_2O_2, or less reactive like $O_2^{\bullet-}$.[20]

Regarding the possible role of $O_2^{\bullet-}$, we have followed the surface degradation in absence or after addition of acid in organic solvent (see eqs 4−7) or at different pH values in water. Figure 3 shows the results obtained after exposure of the

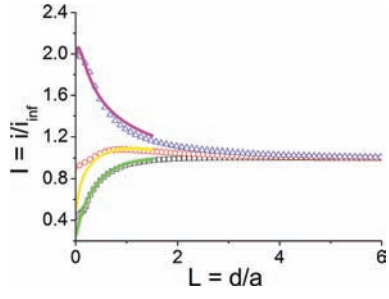

Figure 3. Approach curves recorded with $FcCH_2OH$ 10^{-3} mol L^{-1} as redox probe after exposure to O_2 reduction (2 × 2 s) on a 5 μm radius disk Pt tip electrode. Before adding phenol (black □) and after the addition of 6 × 10^{-3} mol L^{-1} (blue △) and 1 mol L^{-1} (red ○) phenol. Lines are the theoretical curves for k_{el} = 5.2 × 10^{-3} cm·s^{-1} (green line), k_{el} = 10^{-2} cm·s^{-1} (magenta line), and k_{el} = 4.2 × 10^{-2} cm·s^{-1} (yellow line).

sample to O_2 reduction on Pt tip (2 × 2 s)[21] in dry DMF (conditions of stability for superoxide in this media) and when the same experiments are performed after addition of phenol acting as a proton source.[3]

Before adding acid, we noticed that no considerable modification of the surface occurs in dry DMF. When the O_2 reduction is performed in the presence of a small quantity of acid (6 × 10^{-3} mol L^{-1}), the "reading" SECM approach curves evidence the passage from a negative to a positive feedback behavior showing the attack of the surface by ROS.[22] If a large concentration of phenol is added (1 mol L^{-1}), no modification of the surface is then observed. Similar results are obtained in aqueous solution when varying the pH. The modified surface undergoes a low modification under exposure to ROS in 1 mol L^{-1} NaOH solution, a considerable modification in a neutral solution (pH 7.4), and no modification in a 1 mol L^{-1} HCl solution. From this first series of experiments, we could reject that $O_2^{\bullet-}$ is responsible for the transformation of the surface. As seen from eqs 4−7, the reduction of O_2 in the presence of acid leads to the formation of other transient ROS, as $HO_2^{\bullet}$ or H_2O_2. About a possible participation of $HO_2^{\bullet}$, we highlight that reactions 4−6 are fast and thus $HO_2^{\bullet}$ steady-state concentration should remain low.[3] Because of the moderate reactivity of $HO_2^{\bullet}$ versus unsaturated compounds,[23] it is unlikely responsible for the observed phenomena. To assess a possible role of H_2O_2, the sample was immersed in a 30% H_2O_2 aqueous solution for about 30 min. As a result, no degradation of the organic layer was observed. We could thus conclude that neither $O_2^{\bullet-}$, $HO_2^{\bullet}$, nor H_2O_2 is directly responsible for the observed modifications.

As a notable feature, the reduction of H_2O_2 is possible at a Pt electrode at the reduction potential of O_2, which is not the case at an Au electrode.[1,6a] The same observation is made in an organic solvent like DMF, meaning that O_2 reduction at Pt leads to more reduced species (see Figure 4).[24]

To confirm the hypothesis that the ROS responsible for the surface degradation is indeed formed during H_2O_2 reduction, similar footprint SECM experiments were performed using a degassed aqueous H_2O_2 solution (2 × 10^{-3} mol L^{-1}) at neutral pH instead of the aerated O_2 solution. Examination of the exposed sample shows comparable degradations to those observed when O_2 was reduced on Pt electrode confirming that the reactive species is produced at the most reduced states of O_2. If the reduction of H_2O_2 is carried out using Au electrode, no degradation of the substrate is observed showing the special role of Pt surface.

A series of additional experiments were then performed to ensure this conclusion. To reject the possibility that SECM mediator or metallic traces do play a role, another redox couple was tested for reading the surface, tetrathiafulvalene/tetrathiavulfalene radical cation ($TTF/TTF^{\bullet+}$). Exposure to O_2 reduction was also examined without any redox probe present in the solution. Then, the modification of the surface was evaluated in a different solution containing the redox probe. A special care was taken in cleaning of the SECM cell with ultrapure water to remove metallic traces. After taking all these precautions, similar results were always obtained. We could also highlight that the observed transformations of the surface occur in water and in different organic solvents, which makes even more unlikely the presence of common impurities. All these experiments coupled with strong alterations of the surface evidenced by SECM and AFM images (Figure 6) suggest that the reaction with $HO^{\bullet}$ radicals is the most likely pathway. Indeed in the ROS family, $HO^{\bullet}$ appears as the only species able to rapidly react with aromatic compounds.[19]

dx.doi.org/10.1021/ja211663t | J. Am. Chem.Soc. 2012, 134, 2835−2841

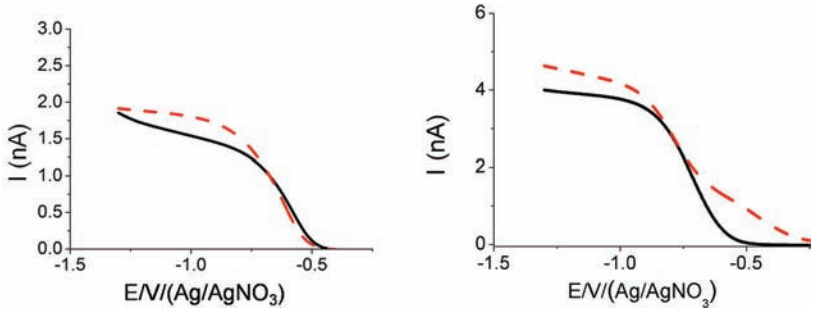

Figure 4. Steady-state voltamograms of O_2 reduction in DMF (0.1 mol L^{-1}) on Au (left) and on Pt (right) before (—) and after addition of 4×10^{-3} mol L^{-1} H_2O_2 (red – – –). Scan rate = 50 mV s^{-1}. Reduction of hydrogen peroxide at the Pt electrode is clearly observable before oxygen reduction, whereas at the gold electrode, the reduction of H_2O_2 occurs at a more negative potential.

Considerations about the Reaction Mechanism. Our experiments show that ORR at Pt surface leads to the concurrent formation of $HO^\bullet$ radicals besides the formation of water. The process appears to be specific to ORR electrocatalysis by Pt and does not occur when O_2 is reduced on another electrode like Au. Starting from molecular O_2, it corresponds to the occurrence of a 3-electron pathway in O_2 reduction (reaction 8) or to the monoelectronic reduction of H_2O_2 (reaction 9):

$$O_2 + 2H^+ + 3e^- \rightarrow HO^\bullet + OH^- \quad (8)$$

$$H_2O_2 + e^- \rightarrow HO^\bullet + OH^- \quad (9)$$

This is an unexpected process even if $HO^\bullet$ production may be envisaged during ORR, for example, in the Haber–Weiss reaction.[1,25] In electrochemical conditions, literature reports the 2-electron reduction of H_2O_2 to water or the transient formation of hydroperoxyl radical $HO_2^\bullet$ that could not be responsible for the degradation as explained above.[1,6a] From a thermodynamic view, $OH^\bullet$ radical production in reaction 8 is possible at the reduction potential of O_2 at neutral pH ($E°$ = +0.39 V/NHE at pH 7).[20a] However, the radical should be rapidly converted to OH^- (or H_2O) ($E°$ = +2.31 V/NHE at pH 7)[20a] at the electrode surface at such negative potential, which is not the case. This may suggest that more efficient radicals are produced in the diffusion layer between the tip electrode and the sample rather than on the electrode surface and that only a small fraction of the produced ROS reach the surface. According to the eq 8, proton source is required. Indeed, we observed that the surface degradation is more efficient in the presence of a moderate concentration of acid in solution (Figure 3). We noticed that higher amounts of added phenol inhibit the surface reaction certainly because produced ROS are trapped before reaching the sample.[19]

Concerning the variation of the reactivity in different media, $HO^\bullet$ reacts with most aromatic or unsaturated compounds (by hydrogen atom abstraction, oxidation, addition) at bimolecular rates approaching the diffusion-controlled limit in aqueous solution.[19] It was recently shown that hydroxyl radical is considerably less reactive in dipolar, aprotic solvents such as acetonitrile,[26] which falls in line with the solvent effect illustrated in Figure 2. Another possible explanation is that despite a lower reactivity, $HO^\bullet$ is still able to react with organic solvents (by H abstraction or addition on unsaturated bond) leading to secondary radicals, peroxy or carbon radicals that could also start chain reactions:[27]

$$HO^\bullet + RH \rightarrow R^\bullet + H_2O \quad (10)$$

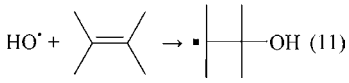

Some of these species are also reactive, but their strength depends on the solvent explaining the noticed efficiency of the patterning in different media. Finally, we should highlight that consequences of $HO^\bullet$ production by electroreduction of O_2 at Pt surface are clearly visible in previously published experiments, even if it was not commented[28] and that reported catalysts instabilities for ORR are certainly related to such a process.[1]

Optimization for Surface Micropatterning. We performed additional experiments in which one parameter was optimized (tip–substrate distance d, pH, applied tip potential for O_2 reduction) during exposure to O_2 reduction (other conditions remain similar, especially the time of exposure to ROS). The changes were then evaluated by recording the approach curves with $FcCH_2OH$ as redox mediator. The first optimized parameter was the tip–substrate distance used during $OH^\bullet$ production. Figure 5 (left) displays the SECM approach curves recorded when ROS are produced at distances d = 3, 10, and 20 μm (L= d/a = 4, 2, 0.6, respectively). It could be observed that the ROS-attack is low at d = 20 μm, while at d = 10 μm and below, transformation occurs in agreement with concentration profiles at the tip microelectrode.[14] A value of d = 3 μm (L = 0.6) appears as a good compromise between the difficulty to control the position of the tip electrode and an efficient modification. The second optimized parameter was the pH value. In acidic media (0.5 mol L^{-1} HCl), the feedback remains negative after O_2 reduction exposure, while in basic media (1 mol L^{-1} NaOH solutions), the surface degradation occurs, but it appears slightly less efficient than in neutral pH. Concerning the value of applied potential at the platinum tip, no modification is observed when the applied potentials remain in the 0 to −0.5 V range. On the contrary, when applied potential is lower than −0.5 V, thus, allowing O_2 reduction, the "reading" approach curves show the transformation of the layer (see Figure 5, right).

On the basis of these parameters, we used the $OH^\bullet$ production to draw different patterns on the surface by displacing the tip during O_2 reduction.[29] Each SECM image was correlated with a corresponding AFM image that was recorded

dx.doi.org/10.1021/ja211663t | J. Am. Chem.Soc. 2012, 134, 2835–2841

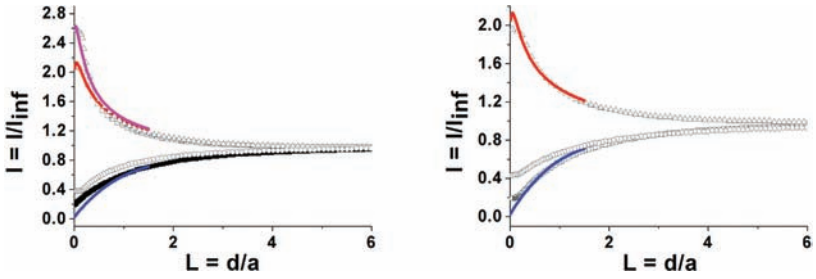

Figure 5. Optimizations of applied potential and tip−sample distance. SECM approach curves (Pt UME, a = 5 μm) on modified GC electrode in H_2O and KPF_6 (0.1 mol L^{-1}). $FcCH_2OH$ (10^{-3} mol L^{-1}) is used as a redox probe. Lines are the simulated curves for electron transfer kinetics. (Left) Effect of distance: before (■) and after the exposure to O_2 reduction of the surface at d = 20 μm (○), 10 μm (□), 3 μm (Δ). k_{el} = 4.7 × 10^{-4} cm s^{-1} (blue line), 3.9 × 10^{-2} cm s^{-1} (red line), 5.0 × 10^{-2} cm s^{-1} (magenta line). d is the tip−substrate distance. (Right) Effect of tip potential: E = −0.5 V (○) and −1.0 (Δ) V vs $Ag/AgNO_3$. k_{el} = 4.7 × 10^{-4} cm s^{-1} (blue line), 4.0 × 10^{-2} cm s^{-1} (red line).

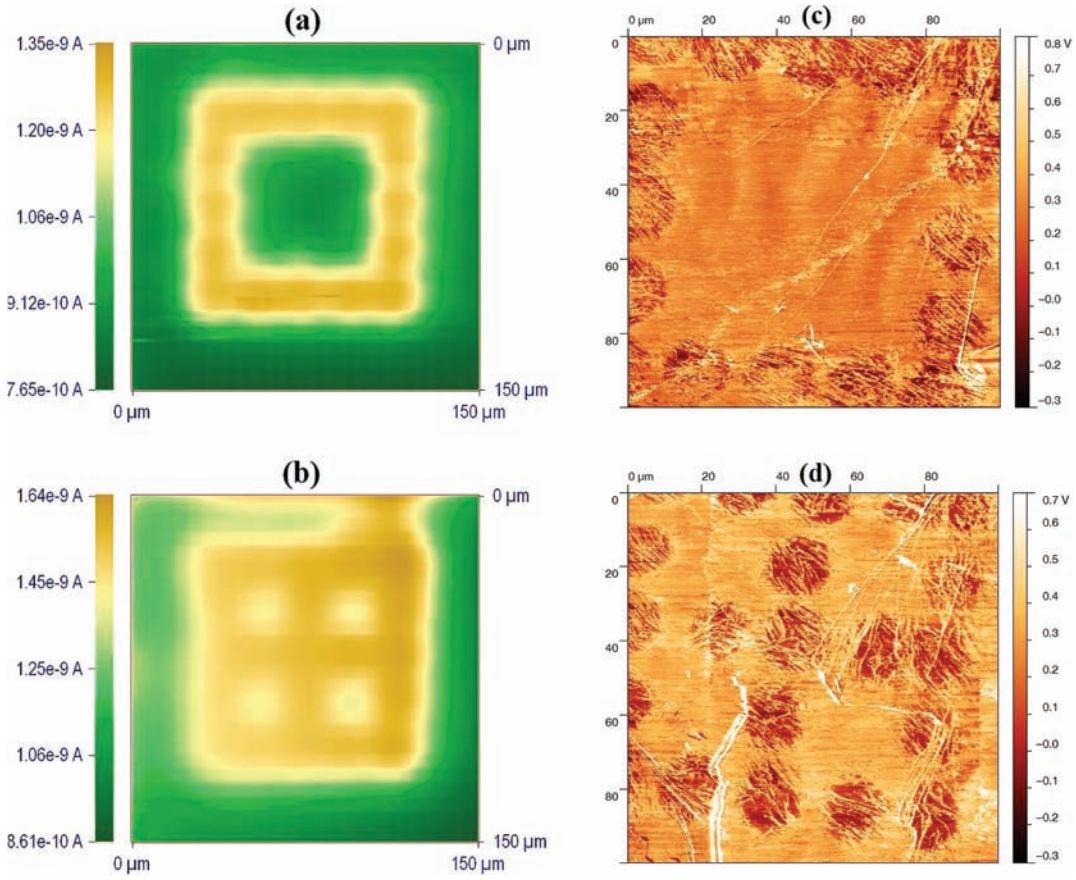

Figure 6. (a and b) SECM images were acquired with a 5 μm radius Pt microelectrode using 10^{-3} mol L^{-1} $FcCH_2OH$ as redox mediator in H_2O/KPF_6 0.1 mol L^{-1} (applied potential −0.8 V vs $Ag/AgNO_3$). Tip velocity, 20 μm s^{-1}. (c and d) AFM images of the localized micropatterning. Images were recorded after micropatterning of the surface with ROS (see text).

under air. AFM images (Figure 6c,d) reveal considerable topological changes due to the destructive effects of ROS versus the organic film anchoring on carbon surface. The size of each produced circular area corresponds to 20 μm diameter using a 5 μm radius Pt microelectrode tip for O_2 reduction. The value was confirmed by SECM imaging.

■ CONCLUSION

SECM shows a considerable production of very active ROS, most likely $OH^•$ radicals, during O_2 reduction on a Pt electrode in water and as a primary radical in organic media. This is a nonclassical process in the sense that a simple reduction leads to the formation of highly oxidative species. If the consequences of OH radicals are observable, the exact mechanism remains unclear and would require additional investigations. When looking in the literature, evidence for this process exist and their consequences are visible on other samples like modified glasses. It is likely that other catalysts proposed for ORR display similar features to Pt. In that sense, the generally admitted description of ORR as simple competitive pathways between 2-electron (O_2 to H_2O_2) and 4-electron (O_2 to H_2O) reductions presents an incomplete description that could not account for the observed phenomena. Our results suggest that radical footprint investigations should be performed in the characterization of new catalysts for ORR in order to evaluate

dx.doi.org/10.1021/ja211663t | J. Am. Chem.Soc. 2012, 134, 2835−2841

the quantity of undesired produced ROS in complement to the measurement of the catalytic efficiency. Because of the high reactivity of $OH^{\bullet}$, "escaping" radicals decrease not only the stability of the electrocatalysts, as often observed in the literature, but the lifetime of the global devices. On the other hand, we have a very simple way for producing highly reactive species. Preliminary experiments show us that considerable amount of highly reactive ROS could simply be produced, using aerated tap water and a Pt microelectrode, opening routes to many practical applications.

AUTHOR INFORMATION

Corresponding Author

philippe.hapiot@univ-rennes1.fr

Notes

The authors declare no competing financial interest.

ACKNOWLEDGMENTS

Prof. Jean Pinson (ESPCI, Paris) is thanked for the gift of benzenediazonium tetrafluoroborate salt.

REFERENCES

(1) (a) Sawyer, D. T.; Valentine, J. S. *Acc. Chem. Res.* **1981**, *14*, 393. (b) Kinoshita, K. In *Electrochemical Oxygen Technology*; John Wiley and Sons: New York, 1992. (c) Adzic, R. In *Electrocatalysis*; Lipkowski, J., Ross, P. N., Eds.; Wiley-VCH: New York: 1998; Chapter 5, p 197.

(2) Bard, A. J. *J. Am. Chem. Soc.* **2010**, *132*, 7559 and references therein.

(3) Andrieux, C. P.; Hapiot, P.; Savéant, J.-M. *J. Am. Chem. Soc.* **1987**, *109*, 3768.

(4) (a) Shao, M.-H.; Liu, P.; Adzic, R. R. *J. Am. Chem. Soc.* **2006**, *128*, 7408. (b) Zang, C.; Fan, F.-R. F.; Bard, A. J. *J. Am. Chem. Soc.* **2009**, *131*, 177.

(5) (a) Costentin, C.; Evans, D. H.; Robert, M.; Savéant, J.-M.; Singh, P. S. *J. Am. Chem. Soc.* **2005**, *127*, 12490. (b) Singh, P. S.; Evans, D. H. *J. Phys. Chem. B* **2006**, *110*, 637. (c) Savéant, J.-M. *J. Phys. Chem. C* **2007**, *111*, 2819. (d) Costentin, C.; Robert, M.; Savéant, J.-M. *J. Phys. Chem. C* **2007**, *111*, 12877.

(6) (a) Cofré, P.; Sawyer, D. T. *Inorg. Chem.* **1986**, *25*, 2089. (b) Sánchez-Sánchez, C. M.; Rodrıguez-Lopez, J.; Bard, A. J. *Anal. Chem.* **2008**, *80*, 3254. (c) Sánchez-Sánchez, C. M.; Bard, A. J. *Anal. Chem.* **2009**, *81*, 8094.

(7) Rodrıguez-Lopez, J.; Alpuche-Avilés, M. A.; Bard, A. J. *J. Am. Chem. Soc.* **2008**, *130*, 16985.

(8) (a) Costentin, C.; Robert, M.; Savéant, J.-M. *Chem. Rev.* **2010**, *110*, PR1–40. (b) Costentin, C; Hajj, V.; Robert, M.; Savéant, J.-M.; Tard, C. *Proc. Nat. Acad. Sc.* **2011**, *108*, 8559.

(9) See for example: Snir, O.; Wang, Y.; Tuckerman, M. E.; Geletii Y.V. Weinstock, I. A. *J. Am. Chem. Soc.* **2010**, *132*, 11678 and references therein.

(10) Most of the literature studies rely on this procedure. For a recent example see Zheng, Y.; Jiao, Y.; Chen, J.; Liu, J.; Liang, J.; Du, A.; Zhang, W.; Zhu, Z.; Smith, S. C.; Jaroniec, M.; Lu, G. Q.; Qiao., S. Z. *J. Am. Chem. Soc.* **2011**, *133*, 20116.

(11) Brillas, E.; Sires, I.; Oturan, M. A. *Chem. Rev.* **2009**, *109*, 6570.

(12) (a) Shiku, H.; Uchida, I.; Matsue, T. *Langmuir* **1997**, *13*, 7239. (b) Ktari, N.; Poncet, P.; Sénéchal, H.; Malaquin, L.; Kanoufi, F.; Combellas, C. *Langmuir* **2010**, *26*, 17348. (c) Ktari, N.; Combellas, C.; Kanoufi, F. *J. Phys. Chem. C* **2011**, *115*, 17891.

(13) Watson, C.; Janik, I.; Zhuang, T.; Charvatova, O.; Woods, R. J.; Sarp, J. S. *Anal. Chem.* **2009**, *81*, 2496 and references therein.

(14) (a) Bard, A. J., Mirkin, M. V., Eds.; *Scanning Electrochemical Microscopy*; Marcel Dekker: New York, 2001. (b) Amemiya, S.; Bard, A. J.; Fan, F. R. F.; Mirkin, M. V.; Unwin, P. R. *Ann. Rev. Anal. Chem.* **2008**, *1*, 95. (c) Wittstock, G.; Burchardt, M.; Pust, S. E.; Shen, Y.; Zhao, C. *Angew. Chem., Int. Ed.* **2007**, *46*, 1584.

(15) (a) Cornut, R.; Lefrou, C. *J. Electroanal. Chem.* **2007**, *608*, 59. (b) Cornut, R.; Lefrou, C. *J. Electroanal. Chem.* **2008**, *621*, 178.

(16) Pinson, J.; Podvorica, F. *Chem. Soc. Rev.* **2005**, *34*, 429.

(17) (a) Pellissier, M.; Zigah, D.; Barriere, F.; Hapiot, P. *Langmuir* **2008**, *24*, 9089. (b) Noël, J.-M.; Sjöberg, B.; Marsac, R.; Zigah, D.; Bergamini, J.-F.; Wang, A.; Rigaut, S.; Hapiot, P.; Lagrost, C. *Langmuir* **2009**, *25*, 2742. (c) Noël, J.-M.; Zigah, D; Simonet, J.; Hapiot, P. *Langmuir* **2010**, *26*, 7638.

(18) ROS species are then locally electrogenerated by applying to the tip electrode a potential of −0.9 V (plateau current for O_2 reduction) during 10 s and repeated 2 times.

(19) (a) $HO^{\bullet}$ reacts rapidly with aromatic compounds with bimolecular rate constants in the $1-5 \times 10^9$ L mol^{-1} s^{-1}.[19b,c] (b) Anbar, M.; Meyerstein, D.; Neta, P. *J. Phys. Chem.* **1966**, *70*, 2660. (c) Neta, P.; Dorfman, L. M. *Adv. Chem. Ser.* **1968**, *81*, 222.

(20) (a) Nordberg, J.; Arener, E. S. J. *Free Radical Biol. Med.* **2001**, *31* (11), 1287. (b) Koppenol, W. H.; Stanbury, D. M.; Bounds, P. L. *Free Radical Biol. Med.* **2010**, *49*, 317.

(21) Shorter exposition times where used to ensure stability of the superoxide anion in the media. See reference 3.

(22) Electrochemical reduction of O_2 in DMF was performed by applying a tip potential of −1.4 V at Pt UME to ensure fast electron transfer at the UME.

(23) (a) Reported values for bimolecular rates in water are in the 10^4-10^5 L mol^{-1} s^{-1} range.[23b−d] (b) Greenstock, C. L.; Ruddock, G. W. *Photochem. Photobiol.* **1978**, *28*, 877. (c) Fujimori, K.; Nakajima, H. *Biochem. Biophys. Res. Commun.* **1991**, *176*, 846. (d) Nadezhdin, A.; Dunford, H. B. *J. Phys. Chem.* **1979**, *83*, 1957.

(24) A partial passivation of the Pt tip upon O_2 reduction is often observed, while this does not occur on an Au electrode.

(25) (a) The Haber–Weiss reaction could produce $OH^{\bullet}$ from H_2O_2 and $O_2^{\bullet-}$. However, this reaction is very slow without a catalyst, notably Fe^{2+}.[25b] (b) Koppenol, W. H. *Redox Rep.* **2001**, *6*, 229.

(26) Mitroka, S.; Zimmeck, S.; Troya, D.; Tanko, J. M. J. *J. Am. Chem. Soc.* **2010**, *132*, 2907.

(27) Jovanovic, S. V.; Jankovic, I.; Josimovic, L. *J. Am. Chem. Soc.* **1992**, *114*, 9018 and references therein.

(28) In Figure 4a from reference 12a, the degradation of a modified glass occurs when the glass is exposed to the reduction of O_2 on Pt in water without added iron.

(29) Patterns on Figure 6a,b were obtained after electrogeneration of ROS in aerated water during 1 s, repeated 4 times in 16 different points for 6a and in 21 different points for 6b, each spaced 20 μm forming a square and a window shape. Obtained arrangements were read by SECM (using $FcCH_2OH$ as redox probe).